J Solid State Electrochem (2008) 12:181–192
DOI 10.1007/s10008-007-0379-0

ORIGINAL PAPER

The effect of magnetic fields on the electrodeposition of iron

Jakub Koza · Margitta Uhlemann · Annett Gebert · Ludwig Schultz

Received: 15 March 2007 / Revised: 30 March 2007 / Accepted: 14 June 2007 / Published online: 11 July 2007

Abstract The effect of a uniform magnetic field with flux density up to 1 T on the electrodeposition of Fe from sulphate electrolyte has been investigated under different field configurations relative to the electrode surface. Voltammetric and chronoamperometric experiments have been carried out coupled with an electrochemical quartz crystal microbalance for in situ mass change measurements. The structure and morphology of the deposited films were determined by scanning electron microscopy, atomic force microscopy and X-ray diffraction measurements. Results show that, when the magnetic field is applied parallel to the electrode surface, the limiting current density and the deposition rate are increased due to the magnetohydrodynamic effect. The nucleation process is also affected in parallel configuration; the current density of the maximum on the chronoamperograms is decreased, and an additional nucleation step might be observed. This effect is attributed to the hydrodynamic response of the electrochemical system. No significant influence on the electrochemical reaction was observed when a magnetic field was applied perpendicular to the electrode. But in this configuration, the morphology of deposited layers is changed by the magnetic field. The morphology changes are discussed. No effect of the magnetic field on the crystallographic structure was observed.

Keywords Iron · Electrodeposition · Magnetic field · Surface morphology · Nucleation

J. Koza (✉) · M. Uhlemann · A. Gebert · L. Schultz
Leibniz Institute for Solid State and Materials Research Dresden,
P.O. Box 27 01 16, 01171 Dresden, Germany
e-mail: J.Koza@ifw-dresden.de

Introduction

The influence of external magnetic fields on electrochemical reactions has been extensively studied during the past decades [1–4]. It has been shown that superimposed magnetic fields influence mainly the rate of mass transport of ions and thus, can affect the morphology and the texture of the deposit [2, 3, 5–14]. Meanwhile, magnetic field effects on electrochemical reactions are widely accepted and summarised in various reviews [1, 15, 16]. The known magnetic forces affecting the mass transport in the electrolyte are: Lorentz force $\vec{F}_L$, field gradient force $\vec{F}_{\nabla B}$, paramagnetic force $\vec{F}_p$.

The Lorentz force $\vec{F}_L$ acts on moving ions in a magnetic field and appears when magnetic field lines cross the electric field lines (Eq. 1):

$$\vec{F}_L = \vec{j} \times \vec{B} \tag{1}$$

where: $\vec{j}$ is the local flux of ions and $\vec{B}$ is the magnetic flux density.

$\vec{F}_L$ acts in the hydrodynamic layer and is accepted as the main driving force of the so-called magnetohydrodynamic (MHD) effect, i.e. an enhanced convection in the magnetic field. For diffusion limited processes the MHD effect causes a reduction in the diffusion layer thickness and an increase in the limiting current density $i_{\lim}$ [2, 4–7, 13, 16, 17]. Aogaki et al. [18] showed by solving Navier–Stokes equation that the limiting current density increases proportional to $c^{*3/4}B^{1/3}$ (Eq. 2) and this has been confirmed by other authors [4, 13, 19]:

$$i_{\lim} = 4.3 \cdot 10^3 \cdot n^{3/2} A^{3/4} D \nu^{-1/4} c^{*4/3} B^{1/3} \tag{2}$$

where: n is the number of electrons involved in the electrochemical reaction, A is the surface area of the electrode, D is the diffusion coefficient of electroactive species, ν is the

viscosity of the electrolyte, c^* bulk concentration of electroactive species in the electrolyte solution, B is intensity of applied magnetic field (parallel to the electrode surface).

Different semi-empirical models have been proposed, but most of the correlations between $i_{\lim}$ and the magnetic flux density B are power functions, $i_{\lim} \sim B^b$, where b is in the range of 0.25 to 1.6 [2, 4, 11, 18, 20].

The field gradient force $\overrightarrow{F}_{\nabla B}$, which acts on magnetic ions to move them in the magnetic field gradient [12, 21], and the paramagnetic force $\overrightarrow{F}_p$ are generated by a magnetic field, acting on the magnetic ions creating local energy density (Eq. 3). Both are independent of the direction of applied magnetic field.

$$E = -\chi_m \frac{B^2}{2\mu_o} c^* \tag{3}$$

where: χ_m is the molar susceptibility of ions, μ_o is the permeability of a free space.

The paramagnetic force $\overrightarrow{F}_p$ was proposed by O'Brien and Santhanam [22] and Waskaas and Kharkaas [23]. They observed that a uniform magnetic field acts on the electrolyte volume containing magnetic ions. When a gradient of the magnetic susceptibility occurs, as it does in the case of electrodeposition processes, it is supposed that the magnetic field causes an additional convection in the diffusion layer. The direction of $\overrightarrow{F}_p$ depends on the properties of the ions. According to (Eq. 4), $\overrightarrow{F}_p$ has the same direction as the gradient of the paramagnetic ions ∇_c. Thus, in the case of electrodeposition paramagnetic ions are pushed away from the surface and diamagnetic ions are attracted to the electrode surface.

$$\overrightarrow{F}_p = \chi_m \frac{B^2}{2\mu_o} \nabla_c \tag{4}$$

Enhanced convection during electrodeposition of paramagnetic ions in a uniform magnetic field caused by $\overrightarrow{F}_p$ was questioned [2]. Hinds et al. [2] compared $\overrightarrow{F}_p$ with diffusion driving force $\overrightarrow{F}_D$ and concluded that the paramagnetic gradient force is negligible and is not expected to play any significant role in mass transport. Leventis and Dass [12] were able to separate $\overrightarrow{F}_p$ from other magnetic forces acting in the electrolyte. They observed that $\overrightarrow{F}_p$ can be stronger then the gravitational force. Recently Coey et al. [24] concluded that there is no first order concentration gradient force acting on diamagnetic or paramagnetic ions in a uniform magnetic field, but that there is a second order correction related with a demagnetizing field. This second order body force is very low and is not expected to be observed in the electrochemical experiments. They suggested that effects observed by [12, 22, 23, 25] are not related with the paramagnetic force, but with the some other magnetic effect like a very small field gradient.

The aim of this work is to analyse effects which are generated by a homogeneous magnetic field with different strength and orientation during iron deposition as well as to characterize the morphology of the deposited layers.

Materials and methods

A schematic drawing of the plating cell is shown in Fig. 1. The electrodeposition was carried out in a three electrode Teflon® cell (Fig. 1). Au (111) sputtered on quartz crystals were used as working electrode and a Pt sheet as counter electrode. The potentiostate (Jaissle) was coupled with a homemade electrochemical quartz crystal microbalance (EQMB). A membrane was used (Nafion®) between the working and counter electrode to prevent oxidation of iron (II) ions [26]. The electrolyte was purged prior of the experiment with nitrogen for about 1h to reduce the oxygen content. All potentials were measured vs a $Hg/Hg_2SO_4/K_2SO_{4(sat.)}$ reference electrode (MSE, 640 mV vs SHE). Depositions were carried out from a electrolyte solution containing 6.5 mM $FeSO_4$ and 0.1 M Na_2SO_4, which was used as supporting electrolyte. A pH value of 3 was adjusted with H_2SO_4.

Cycling voltammetry experiments were performed at a sweep rate of 20 mV/s and the potential range from −750 to −1,650 mV_{MSE}. From the cyclic voltammograms, potentials for the chronoamperometric experiments were chosen, i.e. the potential steps were applied from OCP to −1,500, −1,550 and −1,650 mV_{MSE}.

Homogeneous magnetic fields up to 1 T (HV7, Walker Scientific) have been superimposed during deposition with two different configurations, i.e. parallel and perpendicular to the electrode surface (Fig. 2). All deposition experiments were carried out at room temperature.

The morphology of the deposited layers (~100 nm thick) was analysed with scanning electron microscopy (SEM, FEG Gemini Leo 1530) and atomic force microscopy (AFM, Nanoscope IIIa, Digital Instruments). The roughness was determined with AFM. X-ray diffraction (XRD-XPertPro

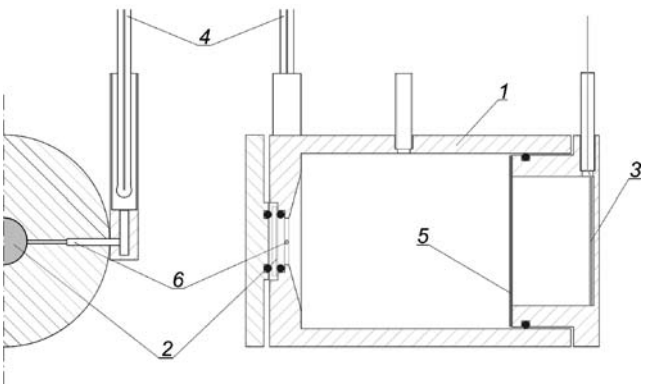

Fig. 1 Schematic illustration of a quartz crystal balance membrane cell. *1*, TEFLON cell, *2*, working electrode (*Quartz*), *3*, Pt counter electrode, *4*, reference electrode ($Hg/Hg_2SO_4/K_2SO_{4(sat.)}$-MSE), *5*, membrane (*Nafion*), *6*, luggin capillary

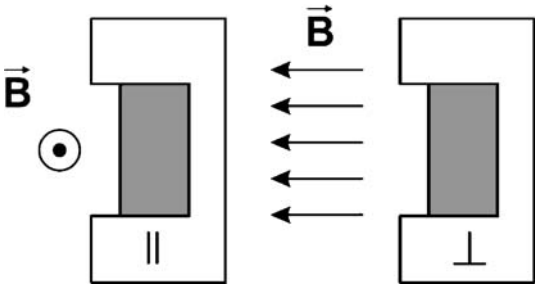

Fig. 2 *B*-field to electrode configurations

Philips) measurements were performed for the determination of the phase composition. The cross-sections of deposited layers were performed with focused ion beam (FIB) and observed under SEM (ZEISS 1540 XP).

Results and discussion

Potentiodynamic polarization

Cyclic voltammetry experiments were carried out with different magnetic flux densities and magnetic-field-to-electrode configurations (Fig. 3). In Fig. 3, cyclic voltammograms and corresponding mass changes for different magnetic flux densities are shown for the parallel configuration (a,b) and for the perpendicular configuration (c,d).

The current density-potential curves show three characteristic peaks in the cathodic region. The first one, at a potential of −1,100 mV_{MSE}, is probably related to the reduction in oxygen [27, 28], which is dissolved in electrolyte despite the N_2-purging. The current density of this peak is increased with increasing magnetic field strength applied parallel to the electrode surface (Fig. 3a). No significant influence was found for the perpendicular configuration (Fig. 3c). It is known that oxygen reduction reaction is in a diffusion-controlled regime [27]. Because of that, the peak current density increase can be explained by increased mass transport due to the MHD effect.

The next peak can be observed at a potential of about −1,400 mV_{MSE} and is related to the hydrogen reduction reaction. The onset of bulk Fe deposition occurs at about −1,460 mV_{MSE}. This is independent of the magnetic field and reaches a maximum at −1,550 mV_{MSE} without magnetic field and with field in perpendicular configuration. It is clearly visible that a magnetic field applied parallel to the electrode surface increases the Fe reduction current and shifts the maximum of the reduction potential to more negative values (Fig. 3a).

The increase in the current densities of the peaks for hydrogen reduction and iron deposition with a magnetic

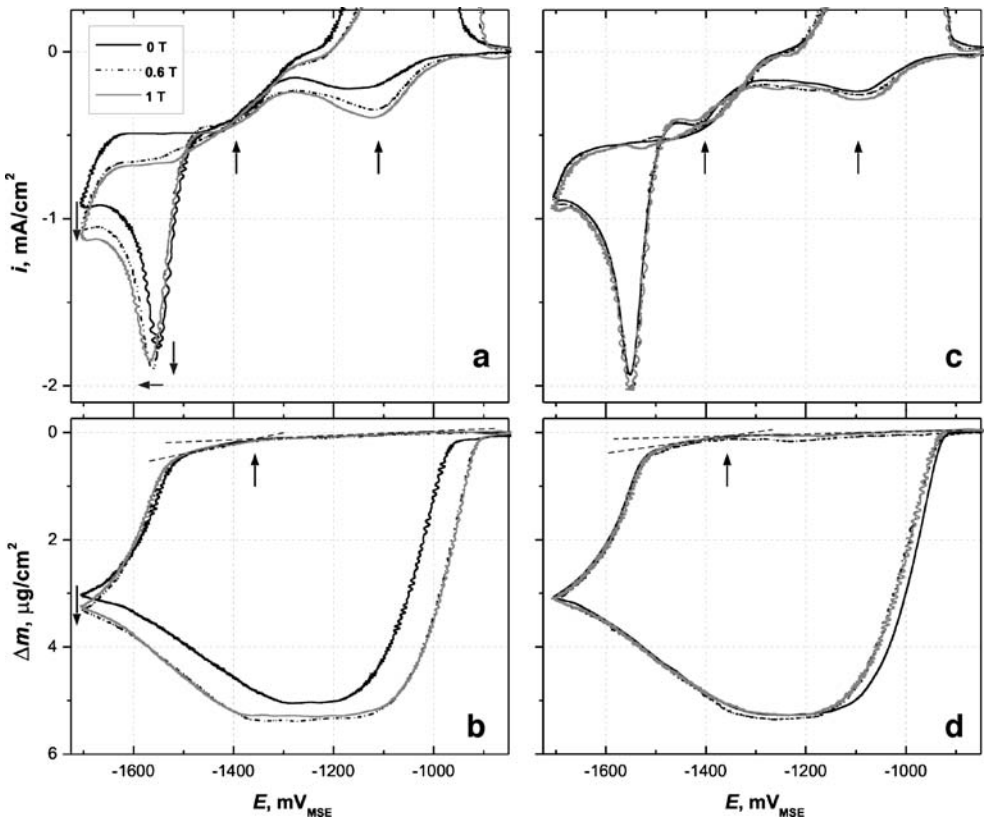

Fig. 3 Cyclic voltammograms (**a**, **c**) and corresponding mass changes (**b**, **d**) of Fe deposition obtained for parallel and perpendicular configuration respectively; d*E*/d*t*=20 mV/s

field applied in parallel configuration can also be explained by the MHD effect, as both reactions are diffusion-controlled [29].

Mass growth is observed from the potential of ca. −1,350 mV_{MSE}, which is independent of the magnetic field strength (Fig. 3b,d). The calculated equilibrium potential from the Nernst equation with the used electrolyte is −1,265 mV_{MSE}, which is more positive than the measured one. The difference is caused by the total overpotential. After this point the mass increases linearly until −1,460 mV_{MSE}. In this potential range, the reduction in hydrogen $\left(E_{H/H^+} = -756\,mV_{MSE}\right)$ is superimposed. Until −1,600 mV_{MSE}, the deposition of Fe dominates, and after this potential the decomposition of water and the hydrogen reduction is the main reaction. It is obvious from Fig. 3b that the total deposited mass is higher when magnetic field is applied in the parallel configuration, but no significant effect was observed for the perpendicular configuration (Fig. 3d). This behaviour corresponds to the back scan of the cyclovoltamogram in Fig. 3a, which shows also an increase in the limiting current density with an increasing B, but no effect for the perpendicular configuration was observed (Fig. 3c). The increased limiting current densities and deposited masses with increasing magnetic field in parallel configuration are in good agreement with the classical MHD effect, which is generally accepted [2, 4–7, 13, 16, 17].

Potentiostatic deposition

Chronoamperometric investigations were performed with different magnetic flux densities and configurations. The deposition potentials were chosen from cyclic voltammograms (Fig. 3a,c) as follows: −1,500 mV_{MSE}, −1,550 mV_{MSE} and −1,650 mV_{MSE}. Fig. 4a,b show the $i(t)$ and corresponding $\Delta m(t)$ transients for the deposition at −1,550 mV_{MSE} with different magnetic intensities in parallel to electrode configuration and Fig. 4c,d with perpendicular to electrode configuration. A stationary regime is reached independently of the magnetic field above 50 s.

It is obvious that a parallel magnetic field increases the limiting current density and deposited mass after 70 s. Such a result is again in good agreement with the classical MHD theory, i.e. additional convection is induced due to the Lorentz force (Eq. 1) acting in the hydrodynamic layer. As a result, the diffusion layer thickness (for mass controlled reactions) is reduced and the limiting current density is increased.

In contrast, if a magnetic field is applied in the perpendicular to electrode configuration no significant effect on $i(t)$ transients was observed (Fig. 4c). In the case of mass changes (Fig. 4d) no significant effect was observed up to 40 s, after that the deposited mass is slightly reduced.

In $\Delta m(t)$ curves (Fig. 4b,d), independently of the magnetic field parameters, linear dependence is reached

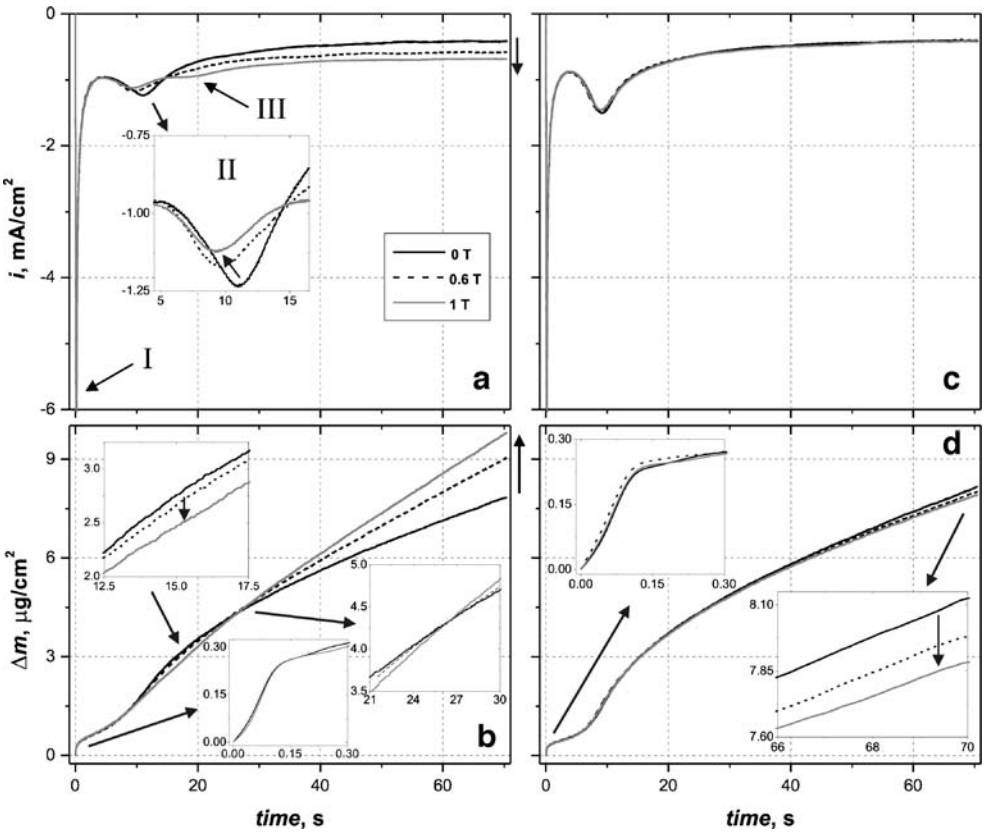

Fig. 4 Chronoamperometric response (**a**, **c**) and corresponding mass changes (**b**, **d**) of Fe deposition obtained for parallel and perpendicular configuration respectively; −1,550 mV_{MSE}

after 50 s of deposition, which is in good correlation with the $i(t)$ transients and reflects the steady state conditions.

In Fig. 4a,c interesting nucleation phenomena can be observed at the beginning of the deposition step (5–15 s) where a second current density maximum is observed (II). In the case of the magnetic field applied parallel to the electrode surface (Fig. 4a), the magnetic field reduces the current density of this peak and shifts it to shorter times. No such effect was observed for the perpendicular configuration (Fig. 4c). This is an influence of the magnetic field opposite to the one, which was expected, i.e. increased current density with applied magnetic field. This effect is also visible in the $\Delta m(t)$ curves (Fig. 4b), i.e. magnetic field decreases the deposited mass in the early beginning of the deposition step, then this dependence is reversed (~27 s), and the expected increase is observed. A similar effect on the deposited mass was found for Cu deposition from low concentration electrolyte [29].

Figure 5 shows the magnetic field dependence of the current enhancement for iron partial current densities (Fig. 5a) and for the hydrogen evolution reaction (Fig. 5b). The iron partial current density was calculated from the deposited mass and applying a graphical differentiation of the $\Delta m(t)$ transients (Fig. 4b,d; Eq. 5). The hydrogen partial current is the difference between the measured current density and the partial current density for iron calculated from the mass.

$$i = \frac{dm}{dt} \cdot k_{Fe}^{-1} \tag{5}$$

where: i is the current density, t is time, m is mass, k_{Fe} is the electrochemical equivalent of iron.

Typical example curves are shown in Fig. 8. The current enhancement parameter was used for making the magnetic field influence evident because it is very sensitive even for small differences:

$$\text{current enhancement} = \frac{i_{\mathrm{lim}}^{B} - i_{\mathrm{lim}}^{0}}{i_{\mathrm{lim}}^{0}} \cdot 100\% \tag{6}$$

where: i_{lim}^{0} is the limiting current density obtained without magnetic field, i_{lim}^{B} is the limiting current density obtained with superimposed magnetic field.

It is obvious that a magnetic field parallel to the electrode surface leads to a stronger current enhancement, i.e. it changes almost linearly for both reactions. The potential dependence is opposite for iron and hydrogen reduction (HER), the highest increase for the Fe reduction (up to ~100%, B=1T) is observed at −1,650 $\mathrm{mV_{MSE}}$ (Fig. 5a). At the same time at this potential the lowest current enhancement for the hydrogen evolution is obtained (Fig. 5b) in the whole magnetic flux densities range in this configuration.

When a magnetic field is applied perpendicular to the electrode surface, 10% retardation of the Fe reduction reaction has been observed for 1 T and −1,550 $\mathrm{mV_{MSE}}$ (Fig. 5a). In the perpendicular configuration for all potentials a retardation of HER occurs at low B (<0.6 T), before a slight enhancement (<10%) is observed at high fields (>0.6 T). However, the retardation of HER is the lowest at the potential (−1,550 $\mathrm{mV_{MSE}}$), where the Fe reduction is most inhibited (Fig. 5b). A similar effect was observed by O'Reilly et al. [7] for the Cu deposition.

To determine the magnetic field influence on the deposited mass under steady state conditions, deposition rates from the linear parts of $\Delta m(t)$ transients (Fig. 4b,d) were plotted vs magnetic flux densities (Fig. 6).

From Fig. 6 it is obvious that the deposition rates of Fe show in linear dependence on the magnetic flux density at all examined potentials. The slopes of those linear

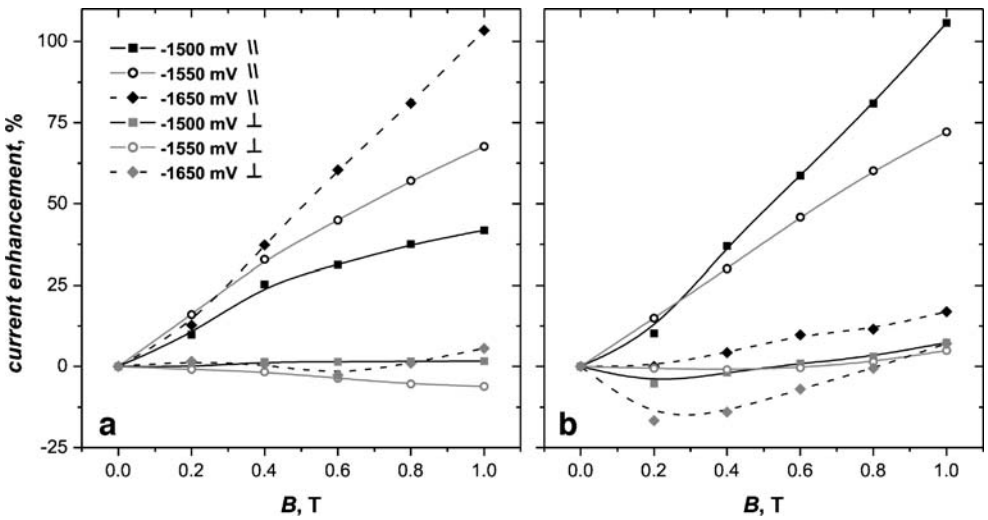

Fig. 5 Current enhancement changes with magnetic field obtained for iron (**a**) and hydrogen (**b**) reduction at used potentials and *B*-field to electrode configurations

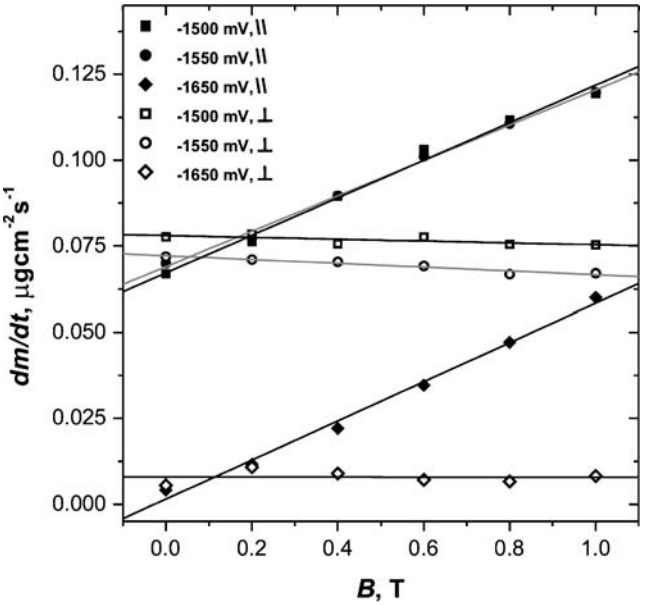

Fig. 6 Deposition rates (slopes of the linear parts of the $\Delta m = f(t)$ plots in Fig. 4b,d.) in dependence on the magnetic flux density and the *B*-field-to-electrode configurations obtained with applied potentials

dependencies are direct proof of influence of the magnetic field on deposition rates (Table 1).

And again it is obvious that magnetic fields in parallel configuration increase the deposition rates due to the MHD effect. In the case of perpendicular configuration it seems that the deposition rates are slightly retarded by the magnetic field, as it was also observed in Fig. 4d.

Because of the small values of the changes, further investigations are needed with higher magnetic flux densities to achieve larger differences. Alternatively, more sensitive methods like electrochemical impedance spectroscopy have to be used. But still, it was suggested that if a magnetic field is applied in perpendicular-to-electrode configuration, then the Lorentz force is negligible and a paramagnetic force $\overrightarrow{F_p}$ may occur which is

Table 1 Slopes of the d*m*/d*t*=*f*(*B*) plots (Fig. 4)

B-field to electrode configuration	Deposition potential		
	−1,500 mV_{MSE}	−1,550 mV_{MSE}	−1,650 mV_{MSE}
Parallel	0.055	0.051	0.057
Perpendicular	−0.003	−0.005	$-9.3\cdot10^{-5}$

pushing paramagnetic species away from the electrode surface [12, 22, 23]. As a result, a reduction in the deposition rate may occur [25].

As mentioned before, in the early stages of the deposition process interesting nucleation phenomena occur indicated by a second current density maximum in the transients in Fig. 4a,c. This maximum is affected by a magnetic field applied parallel to the electrode surface (Fig. 4a), but no effect is observed with perpendicular configuration (Fig. 4c). Nevertheless, the current density-time transients obtained with and without a superimposed magnetic field show the typical response of a multiple nucleation process with the layer-by-layer growth [30]. It can be seen from Fig. 4a,c that the current density increases rapidly and then decreases gradually due to a diffusion-limited growth until a second nucleation step is observed, which seems to be much slower than the first one. The first nucleation step may be related to the first layer formation (possibly monolayer—insert of the $\Delta m(t)$ curves in Fig. 4b,d). According to [30] a surface is covered with deposit until a monolayer is formed (2D growth). This step seems to be independent of a magnetic field. This model was developed for unbounded electrodes where the edge effects are negligible. But real metallic surfaces possess large number of the bounded areas. Besides that, structural defects like dislocations act as preferred nucleation sites, and the monolayer formation process might be affected by them. The second maximum might be related to 3D multiple nucleation and growth with diffusion control

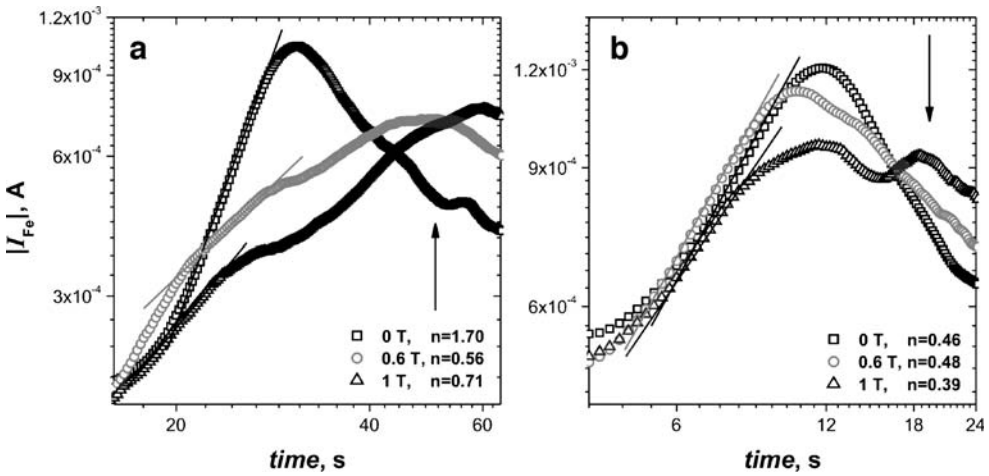

Fig. 7 Logarithmic plots of the Fe partial current vs time with magnetic flux densities **a** −1500 mV_{MSE}, **b** −1,550 mV_{MSE}, parallel configuration

[31]. A similar behaviour with a two step nucleation mechanism was observed for Cu deposition [32].

Figure 7 shows double logarithmic current vs time curves obtained at two different potentials and magnetic flux densities in the parallel configuration for the time range, where the second current maximum occurs. The rising parts of those maxima were used by many authors to derive kinetic information about the electrocrystallisation process [31–35]. It is visible that a magnetic field affects the nucleation process. The current maximum is observed at shorter times and the slope decreases with increasing B. Similar results were obtained for Cu_2O deposition under magnetic fields [36]. Additionally, with superimposed magnetic field a third maximum can be observed (another nucleation step indicated with arrows, Fig. 7).

Different models were proposed resulting from different boundary conditions and used for calculations but most of them were determined as a power function $I \sim t^n$ (or exponential dependencies), from the power parameter it may be possible to determine the nucleation mechanism [33]. But it has to be pointed out that most of those models were developed for isolated deposited nuclei, which do not overlap.

It is not easy to determine any useful kinetic information from the slopes values in Fig. 7, because they are affected by the growth of previous and followed layer, so even the true maximum position is obscured by overlapping layers [30].

It was proposed by Scharifker and Hills [31], that during potentiostatic deposition with 3D multiple nucleation and diffusion-controlled growth two different mechanisms may occur. The progressive nucleation in which nuclei are formed continuously during deposition and the instantaneous in which nuclei are formed on the beginning of the potential step and then grow with the same rate. They proposed that for distinguishing between instantaneous and progressive nucleation mechanism chronoamperometric data can be plotted in the reduced time-reduced current coordinates and compared to the theoretically calculated expressions.

Palomar-Pardave et al. [37] observed for the electrodeposition of cobalt that the co-reduction in hydrogen hinders studies of the deposition process. It is exactly the same in this case—hydrogen reduction affects the current time response what is shown in Fig. 8 where the Fe partial current density was calculated from deposited mass (EQMB). Additionally, the current's maximum time is affected by the previous and following layer growth. The influence of the following layer is especially important in the case of a deposition in a magnetic field, where a third current density maximum occurs and the second current maximum is shifted (Fig. 8b). To reduce the influence of the previous layer, the "zero" time was shifted to the first minimum on the chronoamperogram (Fig. 8, indicated with arrow). The reduced Fe partial current-reduced time chronoamperograms with theoretically calculated dependencies for −1,550 mV_{MSE} with and without applied magnetic field in the parallel configuration are shown in Fig. 9. For the deposition potential of −1,500 mV_{MSE}, it was impossible to determine exact peak positions with the superimposed magnetic field and data are not presented.

From Fig. 9, it is visible that a magnetic field applied during deposition influences the nucleation mechanism. Without magnetic field, deposition seems to be progressive. When a magnetic field is applied, the deposition becomes more instantaneous. In the case of B=1T a third maximum is observed (Fig. 9, another nucleation step indicated with arrow). Experimental data do not fit perfectly to the calculated dependencies. There are many overlapping effects and direction of changes from progressive to instantaneous might be only estimated with

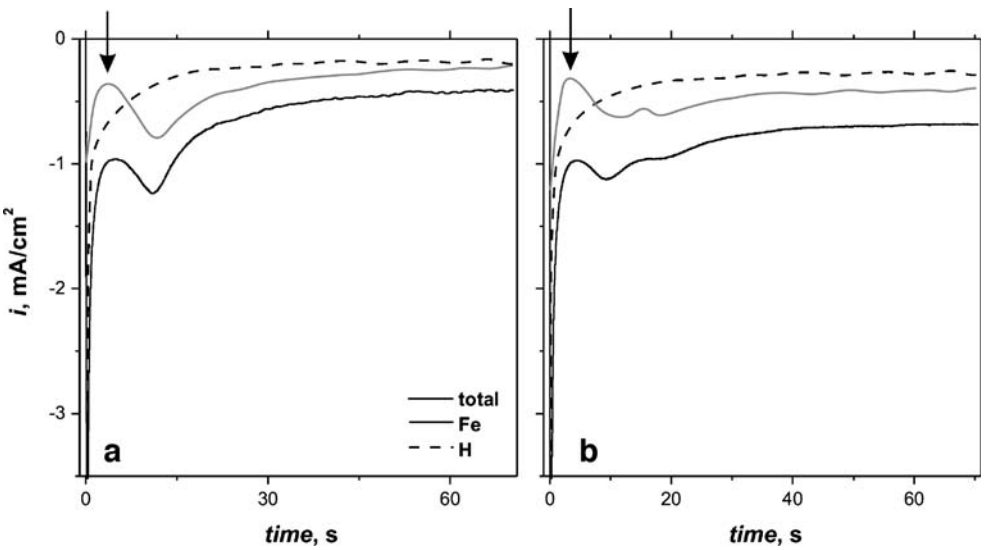

Fig. 8 Current density vs time plots with separated partial current densities for Fe end hydrogen reduction without magnetic field (**a**) and with B=1 T (**b**), −1,550 mV_{MSE}, parallel configuration

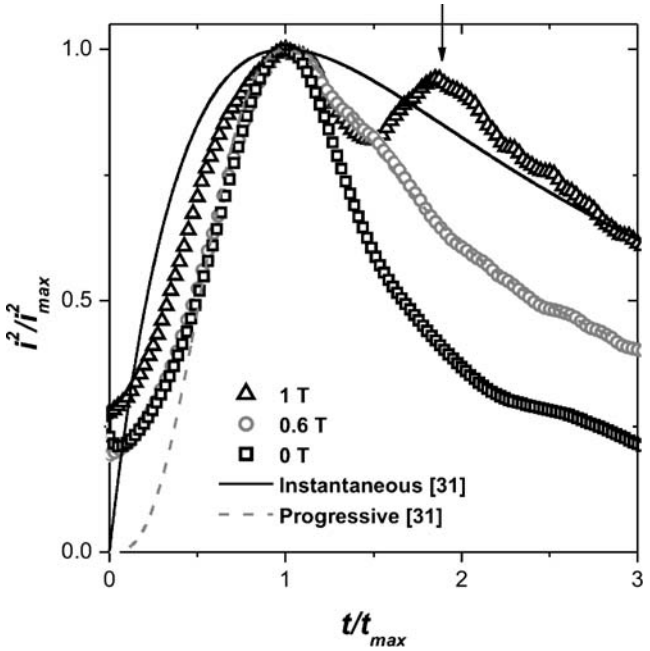

Fig. 9 Reduced Fe partial current-reduced time plots derived from chronoamperograms shown in Fig. 4a as a function of magnetic flux densities, −1,550 mV_{MSE}, parallel configuration

assumption that deposition without applied magnetic field is progressive.

In the case of deposition without applied magnetic field, progressive nucleation occurs which corresponds to a fast growth of nuclei on many active sites (Fig. 10a). Nuclei are formed during the whole nucleation step, nucleation and growth occur simultaneously (Fig. 10b). The current density for separated Fe nucleus is relatively low, but the total current is high because the active surface area is high (relatively high number of nuclei per unit area, which is time dependent, $N(t)=N_oAt$—where: N_o is number of active sites per unit area at $t\rightarrow 0$ and A is the constant nucleation rate).

The change in the deposition mechanism with the magnetic field might explain the decrease in the maximum current density observed at the beginning of deposition (Fig. 4a). When the magnetic field is applied parallel to the electrode surface, a maximum Lorentz force occurs. Nuclei formed at the beginning of this step possess spherical diffusion zones (Fig. 10c), which may overlap. The thickness of the diffusion layer for each nucleus is

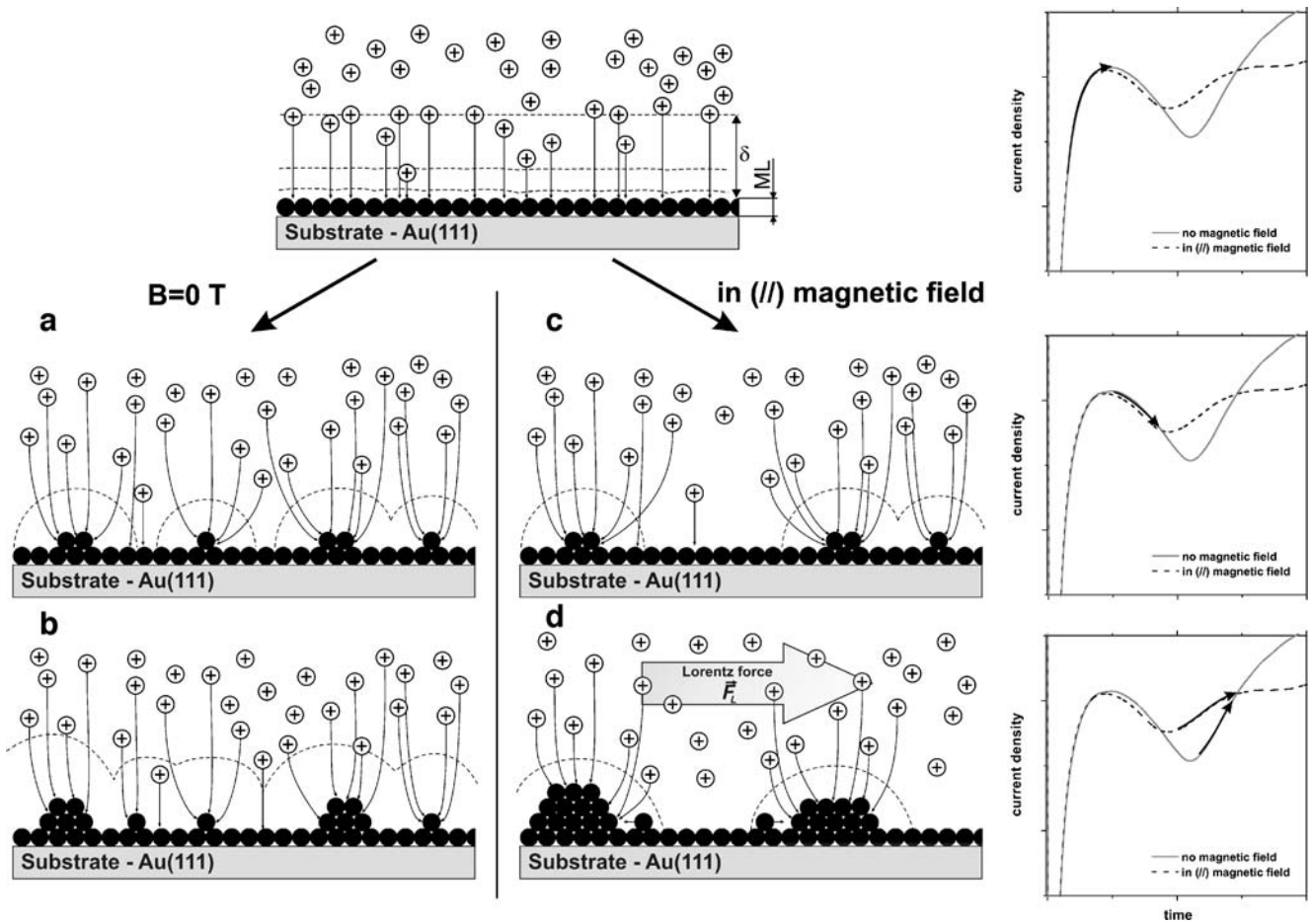

Fig. 10 Schematic presentation of nucleation and growth phenomena at various stages of chronoamperometric experiment without (**a**, **b**) and with superimposed magnetic field in parallel to the electrode surface configuration (**c**, **d**)

reduced due to the MHD effect and thus, the growth rate of the nuclei is enhanced (Fig. 10d). The active surface area for deposition is determined by the total surface of the nuclei during instantaneous deposition. The growth occurs quickly on a relatively small number of active sites that are formed at the early stage of the rinsing part of the current maximum, the current density for separated Fe nucleus is high but the total current of all nuclei relatively low because of the small active surface area (nuclei are formed at the beginning of this step and then 3D growth occurs with a constant rate—relatively low number of nuclei per unit area, N_o).

After a maximum on the current density–time plot occurs, normal Cottrell behaviour is observed which corresponds to a planar diffusion layer with a concentration gradient normal to the electrode surface, and the expected enhancement of the current density with the magnetic field applied parallel to the electrode surface is visible (Fig. 4a).

For better understanding of these phenomena further investigations have to be performed in detail, coupled with microscopic observations.

Structure and morphology

SEM and AFM observations were performed on deposited layers with ~100 nm thickness. Figure 11 shows SEM and related AFM micrographs with the line section analysis of layers obtained at −1,500 mV_{MSE} with and without superimposed magnetic field of 1 T in different configurations. It is clearly visible that for deposits obtained without a magnetic field and with field applied in the parallel configuration grains possess a "leaf"-like shape (Fig. 11a,b,d,e). Deposits obtained without a superimposed magnetic field have a quite compact layer structure with a small porosity randomly distributed over the surface, additionally some holes resulting from hydrogen evolution were found (Fig. 11a). When a

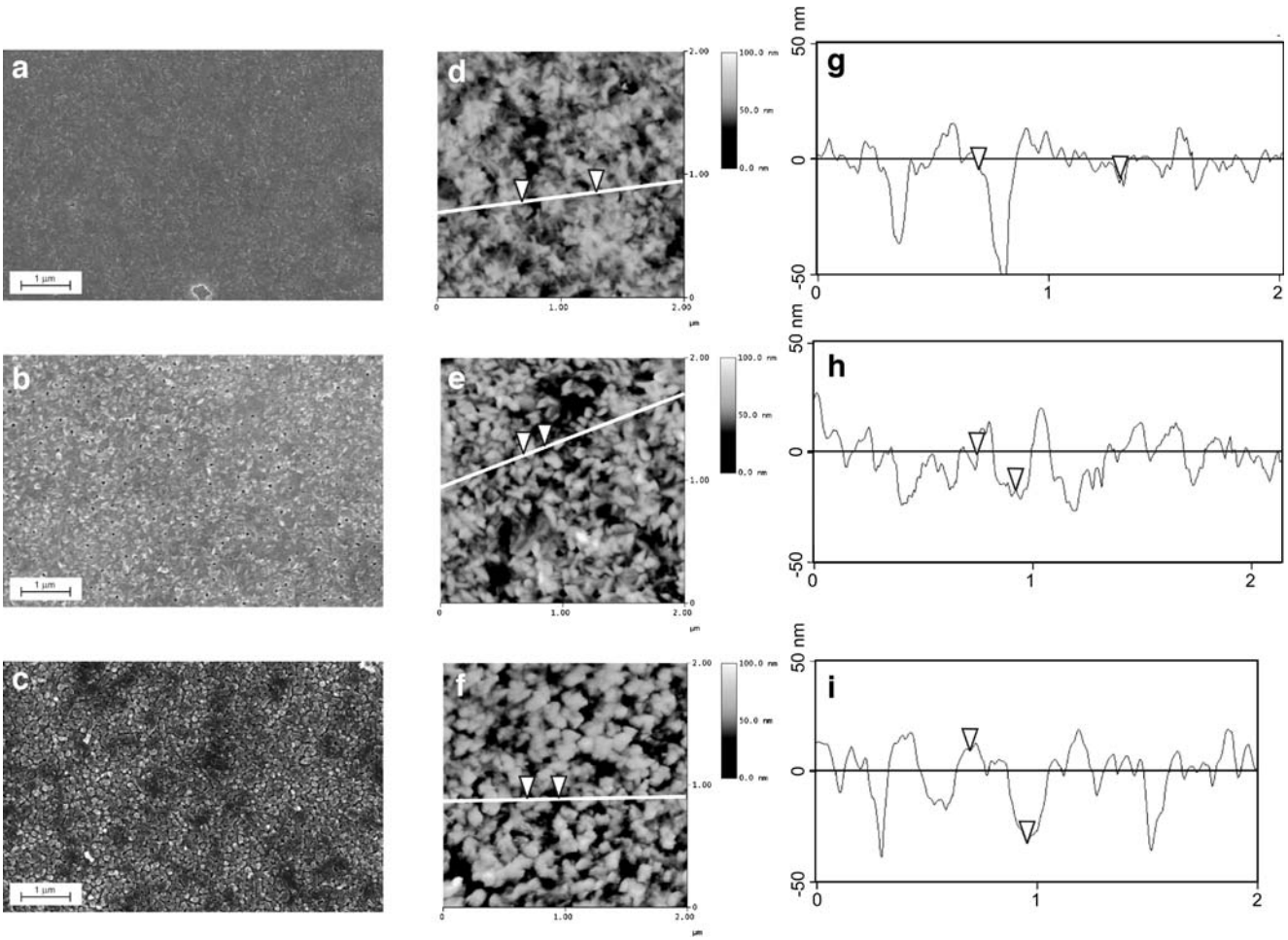

Fig. 11 SEM micrographs and corresponding AFM images with line section analysis of layers (~100 nm) deposited without superimposed magnetic field (**a**, **d**, **g**), B=1 T in the parallel (**b**, **e**, **h**) and perpendicular configuration (**c**, **f**, **i**); −1500 mV_{MSE}

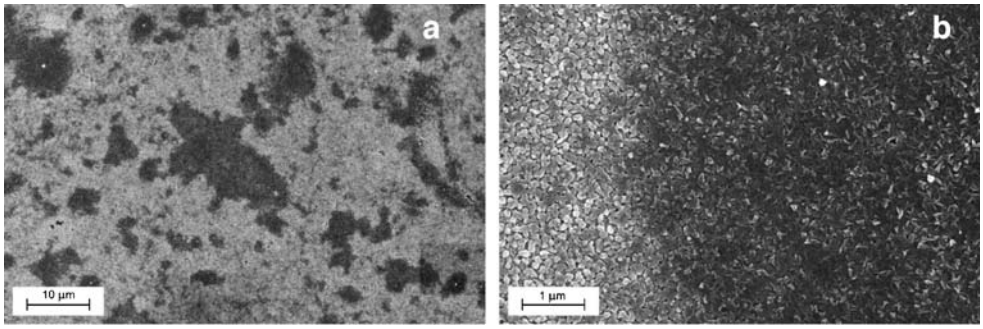

Fig. 12 SEM micrographs of deposited layer (~100 nm) with 1 T magnetic flux density applied in the perpendicular configuration; −1,500 mV_{MSE}

magnetic field is applied parallel to the electrode surface, deposits look more homogenous than those deposited without field, i.e. porosity is uniform on the surface and hydrogen pitting holes were not found, but they possess higher roughness (Fig. 11b,e,h) than those obtained without magnetic field (Fig. 11d,g). Layers deposited with magnetic field superimposed perpendicular to the electrode surface are characterised by a very diverse morphology. The grains shape is polyhedral and grains seem to be oriented perpendicular to the electrode surface (Fig. 11c,f), i.e. in the magnetic field direction. It is also clearly visible, in the line section analysis (Fig. 11i), that deposits obtained in this configuration characterise the highest porosity.

Deposits obtained with magnetic field in perpendicular configuration are very inhomogeneous, dark and light regions (mostly light) can be observed on the surface (Fig. 11). In Fig. 12b, the boundary region between dark and light zone is shown, the dark zone looks identical to deposits obtained without magnetic field. This suggests that the force induced by the magnetic field is not high enough to achieve a perfect distribution on the whole surface.

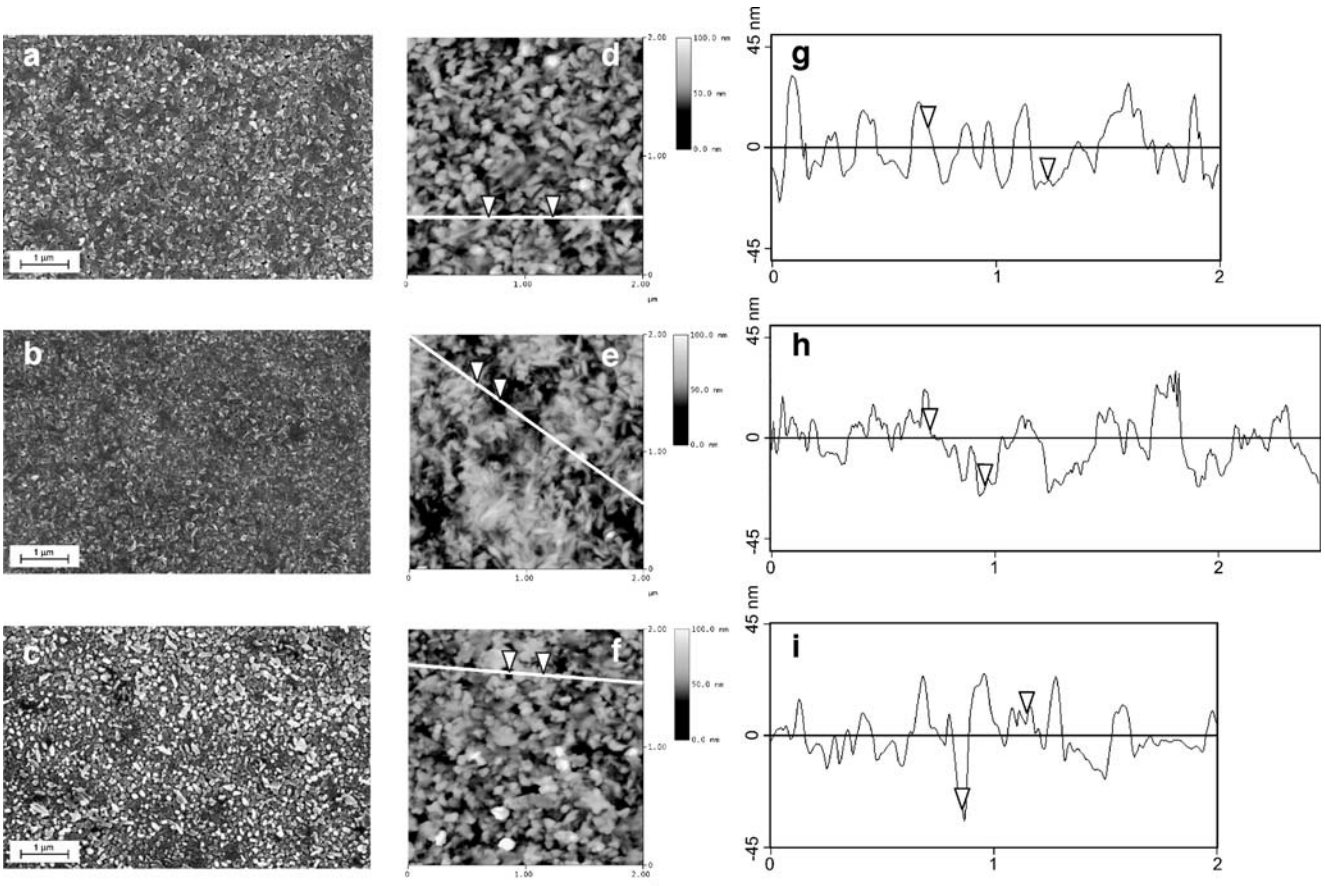

Fig. 13 SEM micrographs and corresponding AFM images with line section analysis of layers (~100 nm) deposited without superimposed magnetic field (**a**, **d**, **g**), B=1 T in the parallel (**b**, **e**, **h**) and perpendicular configuration (**c**, **f**, **i**); −1,550 mV_{MSE}

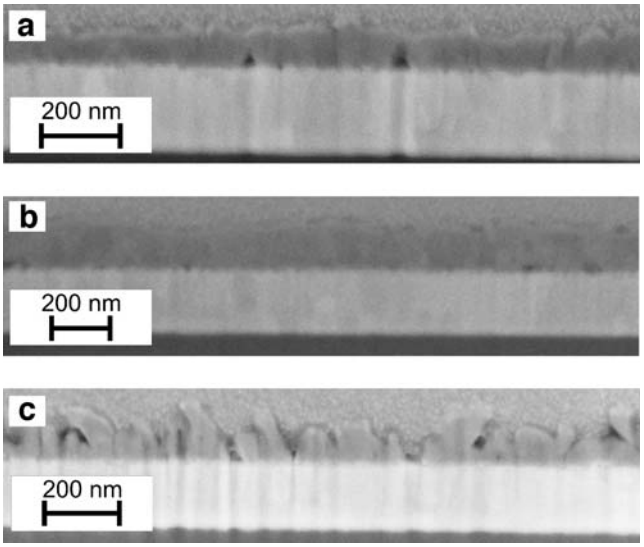

Fig. 14 SEM micrographs of FIB cuts of the deposited layers without, 1 T (//) and 1 T (⊥) magnetic field (**a**, **b**, **c**) respectively; −1,550 mV_{MSE}

In Fig. 13, SEM and related AFM images with line sections analysis of the layers obtained at −1,550 mV_{MSE} with and without superimposed 1 T magnetic field in different configurations are shown. Deposits obtained without magnetic field and with field applied in the parallel configuration look similar to those obtained at −1,500 mV_{MSE}. Grains also possess a "leaf"-like shape (Fig. 13a,b, d,e). But it is clearly visible that the grains are smaller with magnetic field (Fig. 13d,e,g,h). It is also visible that deposits obtained in the parallel magnetic field are more compact with smaller porosity (Fig. 13b,e,h) then those deposited without superimposition of the magnetic field (Fig. 13a,d,g).

When the magnetic field is applied perpendicular to the surface, the morphology obtained at −1,550 mV_{MSE} is also similar to the one obtained at −1,500 mV_{MSE}. The grains are in polyhedral shape and oriented perpendicular to the electrode surface (Fig. 13c,f,i). But the morphology is more homogenous on the whole surface. It might be concluded that the reason is not only a magnetic field effect but it could be an effect of interaction between magnetic and electric field. No significant effect was observed with the electrochemical investigations when magnetic field was applied in the perpendicular configuration (Fig. 4c,d).

Table 2 Roughness (Rms) with standard deviations (S_d) of the deposited layers in dependence of the magnetic field flux density and configuration, obtained at two different potentials

Magnetic flux density and configuration	−1,500 mV_{MSE}		−1,550 mV_{MSE}	
	Rms (nm)	S_d (nm)	Rms (nm)	S_d (nm)
0 T	8.4	1.3	11.9	1.8
1 T, parallel	13.0	1.7	10.6	1.4
1 T, perpendicular	14.8	2.4	13.7	1.1

The perpendicular orientation of the grains is not clearly visible from the surface analysis (Figs. 12 and 13c,f,i), because of that observation of the cross-sections were performed. In Fig. 14, SEM images of the FIB cuts for deposits obtained at −1,500 mV_{MSE} are shown. It is clearly visible that deposits obtained in the perpendicular magnetic field characterize columnar structure with perpendicular to the electrode orientation of the grains (Fig. 14c). This morphology is diametrically opposed to those obtained without (Fig. 14a) and with the parallel magnetic field (Fig. 14b). It is also visible that deposits obtained in the parallel magnetic field are more compact and smoother then those obtained without superimposition of magnetic field (Fig. 14a,b).

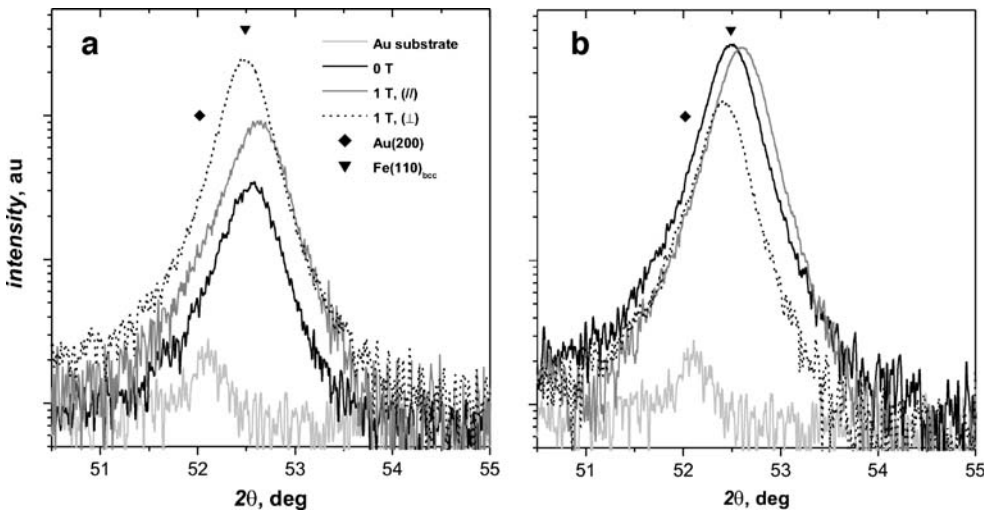

Fig. 15 XRD patterns obtained for layers deposited with and without superimposed magnetic field **a** −1500 mV_{MSE} and **b** −1,550 mV_{MSE}

The roughness of the deposited layers was determined with AFM and are collected in Table 2. In general deposited layers possess a distributed morphology (high values of standard deviations). The magnetic field in the perpendicular configuration increases the roughness independently of the applied potential. The roughness of layers deposited at −1,500 mV_{MSE} is increased with a superimposed magnetic field in both configurations. Similar effect was observed by Krause at al. [29] for Co deposition for low overpotential. Layers deposited at −1,500 mV_{MSE} in applied magnetic fields with parallel configuration exhibit a compact and smooth surface.

The phase compositions of deposited layers were determined by X-ray diffraction measurements. XRD patterns obtained from layers deposited with different magnetic field orientations and B=1 T at two different potentials shows only the main (110) reflex of bcc Fe (Fig. 15a,b). No other reflexes were observed in the range of 2θ angles from 20 to 120°. It is possible that obtained deposits are single-phase, but to prove this further texture investigations are needed.

Conclusions

The effect of superimposed magnetic fields (0–1 T) with parallel and perpendicular orientation relative to the electrode surface on the electrocrystallization of Fe was studied in acidic ferrous sulphate electrolyte at room temperature. General results can be summarised as follows:

A primary effect of magnetic fields on the electrochemical reaction is the MHD effect acting in the bulk electrolyte (parallel configuration), which reduces the diffusion layer thickness and thus, the limiting current densities and deposition rates are increased with a superimposed magnetic field.

The nucleation process is affected by the magnetic field when it is applied parallel to the electrode surface (maximal Lorentz force). This influence is attributed to the MHD effect.

No significant effect of magnetic fields on the electrochemical system was observed when it was applied perpendicular to the electrode surface.

A magnetic field changes the morphology of Fe deposits. Layers deposited under magnetic field applied parallel to the electrode are more homogenous than those obtained without field. In the case of perpendicular configuration grains are oriented perpendicular to the surface, i.e. in the magnetic field direction.

No effect of magnetic fields independently of their flux density and orientation on the crystallographic structure was observed.

Acknowledgements The German Research Foundation (DFG) is gratefully acknowledged for the support of this work in the framework of SFB609 "Elektromagnetische Strömungsbeeinflussung in Metallurgie, Kristallzüchtung und Elektrochemie."

References

1. Tacken RA, Janssen LJJ (1995) J Appl Electrochem 25:1
2. Hinds G et al (2001) J Phys Chem B 105:9487
3. Shannon JC, Gu ZH, Fahidy TZ (1997) J Electrochem Soc 144: L314
4. Lioubashevski O, Katz E, Willner I (2004) J Phys Chem B 108:5778
5. Aaboubi O et al (1990) J Electrochem Soc 137:1796
6. Devos O et al (1998) J Electrochem Soc 145:401
7. O'Reilly C, Hinds G, Coey JMD (2001) J Electrochem Soc 148:C674
8. Tabakovic I et al (2003) J Electrochem Soc 150:C635
9. Nikolic ND et al (2004) J Magn and Magn Mater 272–276:2436
10. Uhlemann M, Schlörb H, Msellak K, Chopart JP (2004) J Electrochem Soc 151:C598
11. Rabah KL et al (2004) J Electroanal Chem 571:85
12. Leventis N, Dass A (2005) J Am Chem Soc 127:4988
13. Uhlemann M, Krause A, Chopart JP, Gebert A (2005) J Electrochem Soc 152:C817
14. Matsushima H et al (2006) J Electroanal Chem 587:93
15. Fahidy TZ (1999) The effect of magnetic fields on electrochemical processes. In: Conway BE et al (ed) Modern aspects of electrochemistry, vol 32. Kluwer/Plenum, New York, pp 333–354
16. Coey JMD, Hinds G (2001) J Alloys Compd 326:238
17. Devos O et al (2000) J Phys Chem A 104:1544
18. Aogaki R, Fueki K, Mukaibo T (1975) Denki Kagaku oyobi Kogyo Butsuri Kagaku 43:504
19. Leventis N, Gao X (1999) J Phys Chem B 103:5832
20. Ragsdale SR, White HS (1999) Anal Chem 71:1923
21. Ragsdale SR, Grant KM, White HS (1998) J Am Chem Soc 120:13461
22. O'Brien RN, Santhanam KSV (1997) J Appl Electrochem 27:573
23. Waskaas M, Kharkats YI (1999) J Phys Chem B 103:4876
24. Coey JMD, Rhen FMF, Dunne P, McMurry S (2007) The magnetic concentration gradient force—is it real? J Solid State Electrochem. DOI 10.1007/s10008-006-0254-4
25. Uhlemann M, Gebert A, Schultz L (2004) Electrochim Acta 49:4127
26. Osaka T et al (2003) Electrochem Solid-State Lett 6:C35
27. Vetter KJ (1961) Elektochemische kinetik. Springer, Berlin Heidelberg New York
28. Wang J (2000) Analytical electrochemistry, 2nd edn. Wiley VCH, New York
29. Krause A (2005) Electrokristallisation von Kobalt und Kupfer unter Einwirkung homogener Magnetfelder. PhD thesis, TU Dresden
30. Armstrong RD, Harrison JA (1969) J Electrochem Soc 116:328
31. Scharifker B, Hills G (1983) Electrochim Acta 28:879
32. Palomar-Pardave M, Gonzalez I, Batina N (2000) J Phys Chem B 104:3545
33. Thirsk HR, Harrison JA (1972) A guide to the study of electrode kinetic. Academic, London and New York
34. Sahari A et al (2006) Catal Today 113:257
35. Bento FR, Mascaro LH (2006) Surf Coat Technol 201:1752
36. Daltin AL, Chopart JP (2005) The effect of magnetic fields on cuprous oxide electrodeposition. In: Proceedings of 6th International PAMIR Conference on fundamental and applied MHD, vol 2, Rigas Jurmala Latvia, pp 179–182
37. Palomar-Padave M, Scharifker BR, Arce EM, Romero-Romo M (2005) Electrochim Acta 50:4736